Lab report Checklist of What's Missing

- □ Title Page

- □ Abstract (0.5 pt)
  - □ Summary
  - □ Key Results & Conclusion

- □ Table of Contents (0.5 pt)

- □ Introduction (1.0 pt)
  - □ What was done?
  - □ Why was it done?
  - □ How was it done?
  - □ Expected Results

- □ Background (Consistent Tense) (2.0 pt)
  - □ Theoretical model
  - □ Cite all Equations

- □ Experimental Procedure (Past Tense) (1.0 pt)
  - □ Equipment list
  - □ Experimental setup figure/drawing
  - □ Procedure

- □ Results & Discussion (Past tense) (2.0 pt)
  - □ Original Data with date & time
  - □ Computed Results & a discussion
  - □ Graphs/Tables are numbered and have a title

- □ Conclusions (Consistent Tense) (1.0 pt)

- □ References (1.0 pt)

- □ Appendices (1.0 pt)
  - □ Sample Calculations
  - □ Raw data

Grade:
Comments:

Experiment 7: Tensile Test Design Project

Antonio Garcia, Mike Hennessy, Jack Michaelis, Tristan Minter

Mechanical Engineering Department

Loyola Marymount University

Los Angeles, California

December 1, 2023

ABSTRACT

Tensile testing is a crucial method in materials science, providing insights into the mechanical properties of materials under tension. This study explores the impact of layer orientation and infill patterns, particularly in 3D-printed Polylactic Acid (PLA), on tensile properties. The experiment involves modifying layer orientation, infill patterns, and other parameters using PrusaSlicer software, followed by testing on an Instron 4050 machine. Various infill patterns (concentric, grid, honeycomb, gyroid, cubic, and rectilinear) are investigated for their influence on tensile strength and ductility. Results indicate that concentric infill patterns exhibit superior ultimate tensile strength compared to grid patterns. Subsequent tests involve modifications to enhance strength, including combinations of infill patterns. The study identifies issues with concentric infill and proposes rectilinear infill as an alternative. The final test reveals that modified rectilinear infill patterns offer improved strain without compromising strength. This research contributes valuable insights into optimizing 3D-printed material properties for diverse applications, from engineering to biomedical fields.

Table of Contents

Introduction

The primary objective of the tensile test design project is to optimize the tensile strength of test samples by strategically manipulating the orientation of fibers and the infill pattern during the 3D printing process. The focus is on harnessing the capabilities of 3D printing to fabricate samples with tailored structural configurations. The approach involves a combination of rectangular and concentric orientations. The motivation behind the lab is material optimization. Understanding the influence of fiber orientation and infill patterns on tensile strength not only contributes to advancing fundamental knowledge in materials science but also holds practical implications for industries relying on high-performance materials. The methodology involves a systematic approach to design and 3D print samples. Many samples are created, and different manipulations are explored, then multiple trials of testing are done to find the strongest samples. The anticipated outcomes include a spectrum of tensile strengths corresponding to different combinations of fiber orientations and infill patterns. Variations in the material's response to tensile forces are expected, shedding light on the optimal configurations for maximizing strength, which is expected to be a combination of concentric and rectangular patterns. The findings from this project could have far-reaching implications across industries reliant on strong and resilient materials. From aerospace engineering to biomedical applications, the optimized configurations identified through this study may help development of more durable and lightweight components.

Background

Tensile Testing

Tensile testing is a fundamental method in materials science used to assess the mechanical properties of materials, particularly their response to stretching or pulling forces. The primary objective of a tensile test is to measure how a material deforms under tension and to determine key characteristics such as ultimate tensile strength, yield strength, and percent elongation. During the test, a standardized specimen of the material is subjected to an increasing load until it reaches the point of failure. The resulting stress-strain curve provides valuable insights into the material's behavior under different levels of applied force, as seen in Figure 1. Tensile testing is widely employed across various industries to evaluate the performance of materials for applications ranging from structural components in engineering to biomedical implants. Understanding a material's tensile properties is crucial for ensuring the safety, reliability, and efficiency of materials in real-world applications [1].

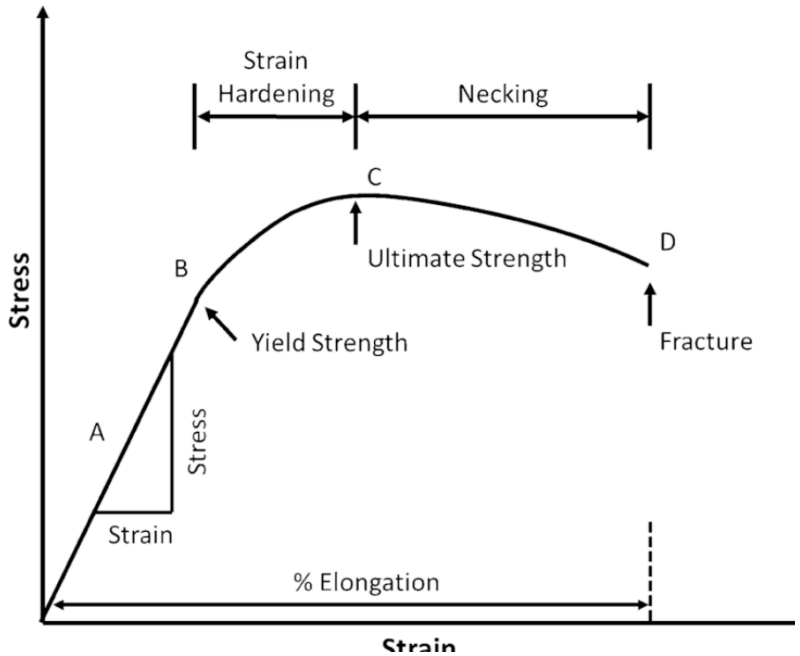

Figure 1: Standard stress vs. strain curve [2].

Polylactic Acid

Polylactic Acid, commonly known as PLA, is a biodegradable and bioactive thermoplastic made from usually corn starch or sugarcane. PLA has gained significant popularity in the field of 3D printing because of its favorable characteristics. It has a low melting point, typically around 180 to 220 degrees Celsius, making it compatible with a wide range of 3D printers. PLA also exhibits good layer adhesion, resulting in smooth and aesthetically pleasing printed objects. However, PLA has limitations, primarily in terms of mechanical strength. While it offers a decent balance of properties for many applications, its relatively low tensile strength may limit its use in high-stress or load-bearing scenarios. This drawback prompts researchers and engineers to explore innovative approaches, such as modifying the printing process, infill patterns, and fiber orientations, to enhance the mechanical performance of PLA-based 3D-printed objects [3].

Layer Orientations

In the realm of 3D printing, layer orientation plays a pivotal role in determining the mechanical properties and overall performance of printed objects. Layer orientation refers to the arrangement and alignment of successive layers during the additive manufacturing process. Figure 2 shows examples of layer orientations. The choice of layer orientation significantly influences the structural integrity, strength, and anisotropic behavior of the printed material. Horizontal layers, commonly parallel to the build platform, are often associated with enhanced mechanical properties in the plane of printing, while vertical layers can contribute to increased strength in the perpendicular direction. Layer orientation's impact on material properties has implications in fields from aerospace to biomedical engineering, where the ability to control strength along different axes is paramount. Understanding and manipulating layer orientation in 3D printing is a key focus in materials science, as it opens avenues for tailoring material characteristics and advancing additive manufacturing technologies [4].

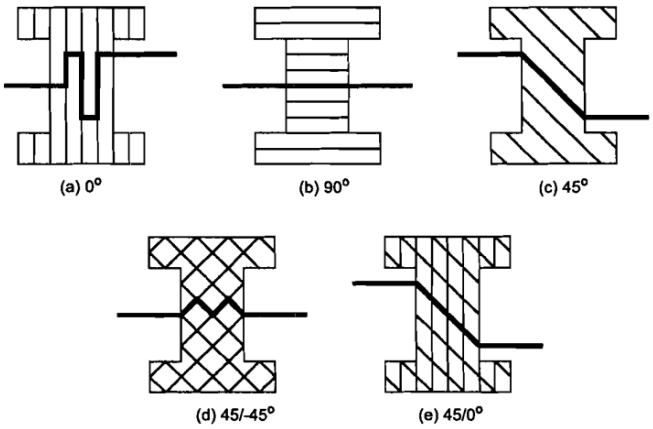

Figure 2: Schematic representation of rupture geometry on ABS samples varying only [4].

Infill Patterns

Infill patterns impact the mechanical properties of 3D-printed materials, influencing their strength, weight, and overall performance. In 3D printing, the infill pattern refers to the internal structure of the printed object, which can vary from solid (100% infill) to sparse arrangements. The choice of infill pattern directly impacts the material's response to mechanical forces, such as tension, compression, and bending. Dense infill patterns, like honeycomb or gyroid, distribute internal support evenly, enhancing structural integrity while minimizing material usage. On the other hand, sparse infill patterns reduce material consumption, making the object lighter but potentially lowering its strength. The infill rate, represented as a percentage, indicates the amount of space filled within the printed object [5, 6]. The following infill patterns are all experimented with during this lab.

Concentric

The concentric infill pattern, as seen in Figure 3, involves filling the interior of a printed object with concentric circles or rings, radiating from the center outward. This simple and visually consistent pattern provides uniform support, enhancing resistance to compression forces. However, it may use more material compared to intricate patterns [5, 6].

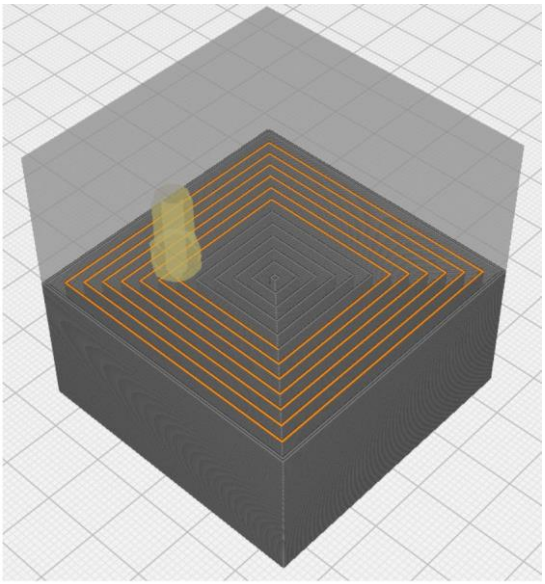

Figure 3: The visual representation of the concentric infill pattern [5].

Grid

The grid infill pattern, as seen in Figure 4, is a structural arrangement where print is filled with a grid of intersecting straight lines. This pattern creates a lattice-like structure, with the lines forming squares or rectangles. Grid infill is known for its balance between structural integrity and material efficiency. The perpendicular orientation of the intersecting lines provides consistent support, distributing internal loads evenly throughout the printed object. This characteristic makes the grid infill pattern effective in enhancing resistance to both compression and tension forces. Furthermore, the simplicity of the grid pattern allows for efficient material usage, striking a practical balance between strength and weight [5, 6].

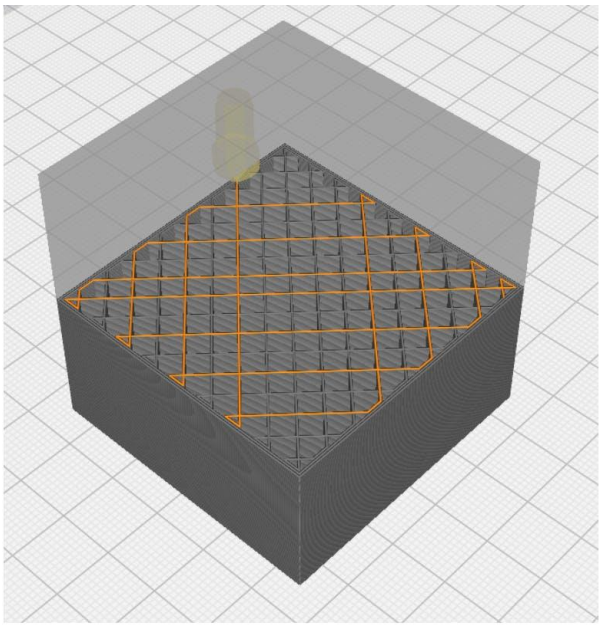

Figure 4: The visual representation of the grid infill pattern [5].

Honeycomb

The honeycomb infill pattern, as seen in Figure 5, involves filling the interior of a printed object with a repeating hexagonal structure, resembling a honeycomb. This pattern is characterized by its balance in structural strength and material usage. The hexagonal cells provide a robust internal framework, distributing loads uniformly and enhancing resistance to both compression and tension forces. The honeycomb infill is known for its lightweight nature, achieved through a combination of geometric efficiency and reduced material volume. The pattern is widely appreciated for its optimal strength-to-weight ratio, making it suitable for applications where both strength and reduced weight are essential [6, 7].

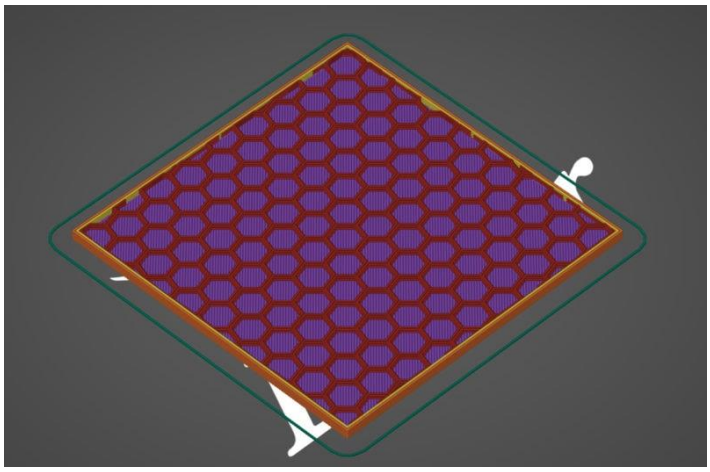

Figure 5: The visual representation of the honeycomb infill pattern [7].

Gyroid

The gyroid infill pattern, as seen in Figure 6, fills the object with a complex, repeating three-dimensional structure that resembles a twisted lattice. The gyroid's interconnected network of pathways provides effective support. What sets the gyroid apart is its intricate geometry, which achieves both strength and lightweight characteristics. The continuous, curved pathways contribute to a unique combination of robustness and material economy. This pattern is particularly advantageous for applications where a high strength-to-weight ratio is crucial [5, 6].

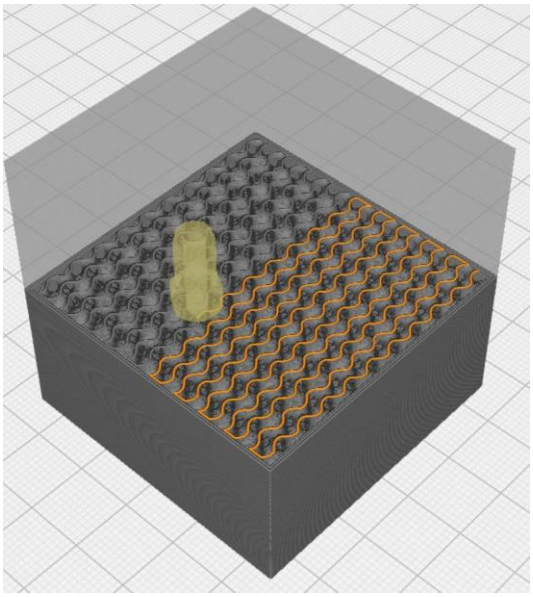

Figure 6: The visual representation of the gyroid infill pattern [5].

Cubic

The cubic infill pattern, as seen in Figure 7, is like the grid pattern, but the straight lines all form cubes. This pattern is recognized for its simplicity and effectiveness in providing structural support. The cubic arrangement forms a lattice-like structure. While the cubic infill is straightforward, its regular geometry makes it reliable for various applications with easy implementation. However, compared to more intricate patterns, it may use more material [5, 6].

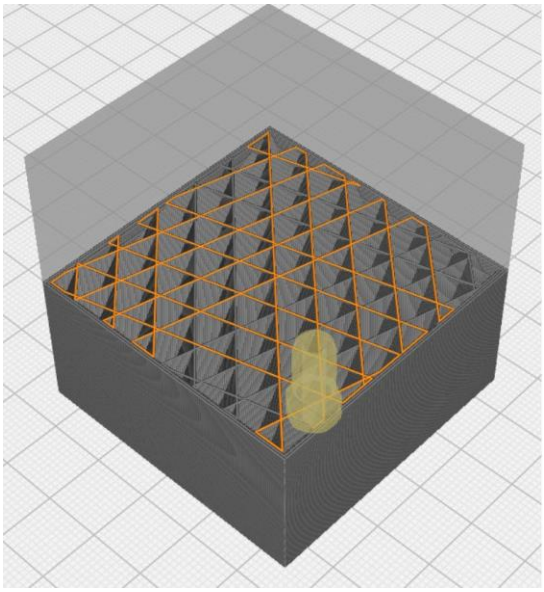

Figure 7: The visual representation of the cubic infill pattern [5].

Rectilinear

The rectilinear infill pattern, as seen in Figure 8, includes a grid of straight, parallel lines that form rectangles. This pattern is characterized by its simplicity and ease of implementation. The straight lines create a basic lattice structure, distributing internal loads uniformly. While the rectilinear infill is straightforward, it may use more material compared to more intricate patterns. The regular grid provides reliable support and is suitable for various applications [6].

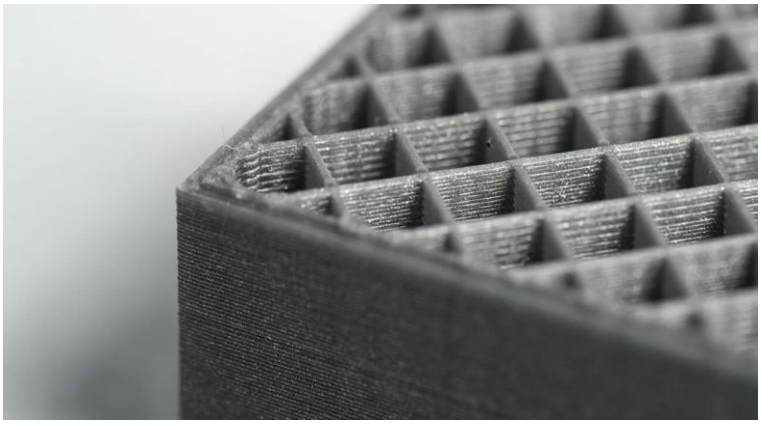

Figure 8: The visual representation of the rectilinear infill pattern [6].

Experimental Procedure

Equipment List:

- Calipers
- Instron 4050
- Blue hill Software on computer connected to Instron 4050
- Extensometer
- Original Prusa i3 MK3S & MK3S+ 3D Printer
- PrusaSlicer Software
- Prusament PLA

Procedure:

1. PrusaSlicer was used to modify the layer orientation, infill pattern, fill density, fill angle and other parameters
2. An SD card was used to transfer the data from PrusaSlicer to the Original Prusa i3 MK3S & MK3S+ 3D Printer
3. The Prusament PLA was restocked, and glue was applied to the hot plate to ensure the samples printed properly on the plate
4. Samples were then removed from the hotplate and tested on the Instron 4050 machine
5. Blue hill Software on a computer connected to Instron 4050 collected data on the elongation and strength of each sample
6. The design was enhanced by repeating steps 1 through 5 until the ductility was as high as can be without compromising too much of the strength of each sample

Experimental Setup:

Instron 4050 was used to perform tensile tests on multiple 3D printed samples with different infill patterns and layer orientations. An extensometer was used to measure the elongation of each sample while it was under tension. Before failure, the extensometer was removed to prevent any damage to the equipment. Figure 9 shows an example of a sample placed into the Instron 4050 machine.

Figure 9: Experimental Setup [8].

A total of 3 trials were conducted where, on average, 3 to 4 samples were tested per trial. During each trial the infill pattern and layer orientation was modified to test how the ductility and strength of the sample changed. The goal was to get as much ductility possible without sacrificing so much strength. Figure 10 shows all the samples that were 3D printed and tested on the Instron 4050 machine.

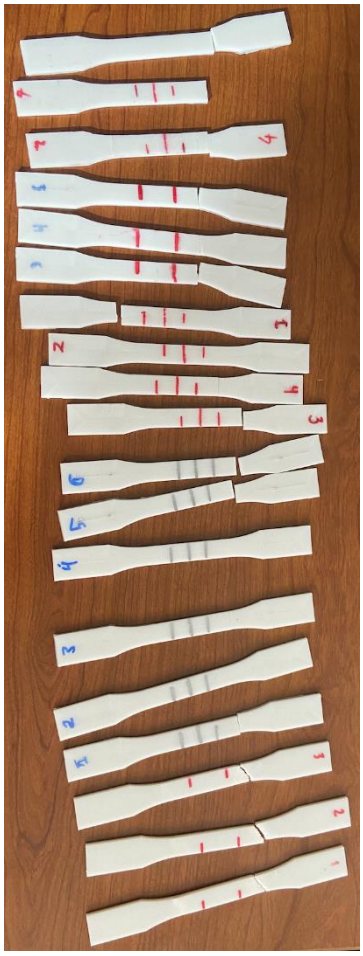

Figure 10: Samples after Tensile Testing [8].

Figure 11: Calipers used to Measure Initial Length and Elongation [9].

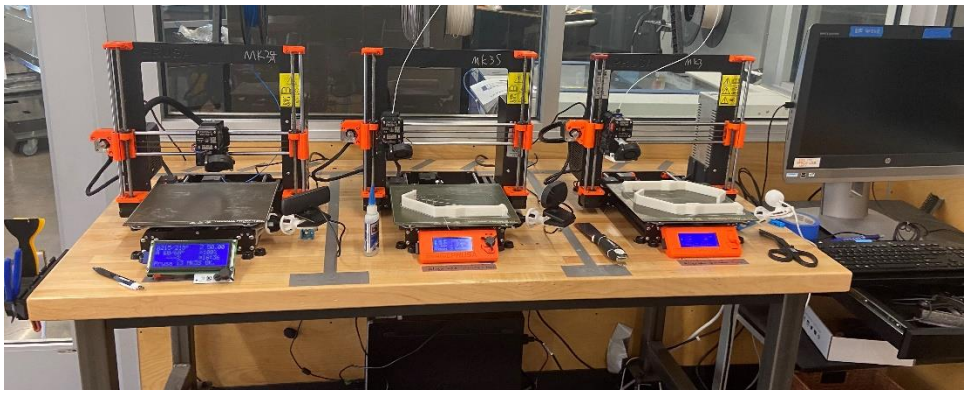

Figure 12: Original Prusa i3 MK3S & MK3S+ 3D Printers [10].

Results and Discussion

In the preliminary examination, two widely adopted infill patterns, namely concentric and grid, were employed. The objective was to assess the respective strengths and weaknesses inherent in each pattern. Results indicated a notably superior ultimate tensile stress for the concentric pattern at 6.788 ksi, compared to the grid pattern's average of 4.825 ksi. Both orientations fractured outside of the marked 1 in area and showed no ductility. The graph below, Figure 13, illustrates the relationship between Tensile Stress [ksi] and Tensile Strain [%], clearly depicting the substantial strength advantage of concentric infill patterns, represented by the red lines on the graph, over the grid infill counterparts.

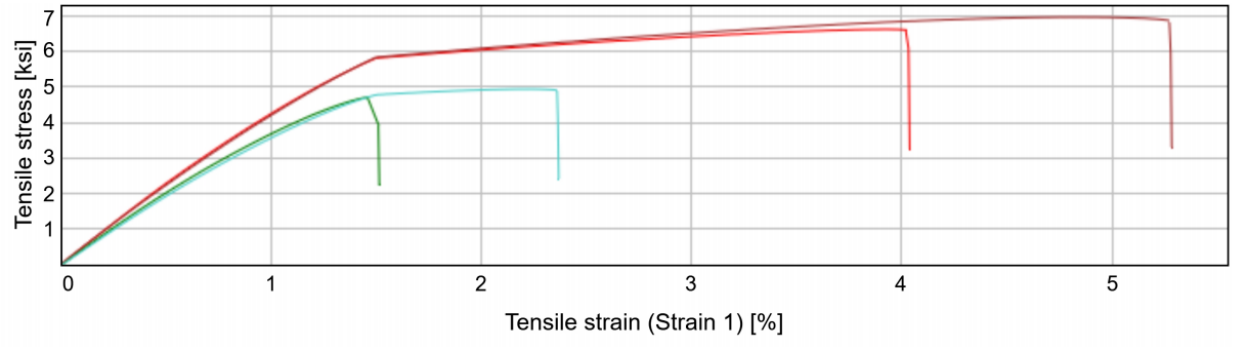

Figure 13: Test 1 Results [8].

As mentioned earlier, the concentric infill pattern served as a solid foundation for subsequent modifications aimed at enhancing strength. The second test primarily involved the individual assessment of the concentric infill pattern along with added layers of angled rectilinear at either the center of the sample or at the ends. As you can see in Figure 14 below all the samples were around the same range of values and exhibited similar properties. The average tensile stress for the three parts tested is 6.139 ksi. Both orientations fractured outside of the marked 1 in area and showed no ductility. However, the third test introduced major modifications to the layering process, aiming to maximize strength within the concentric components using different internal infill patterns.

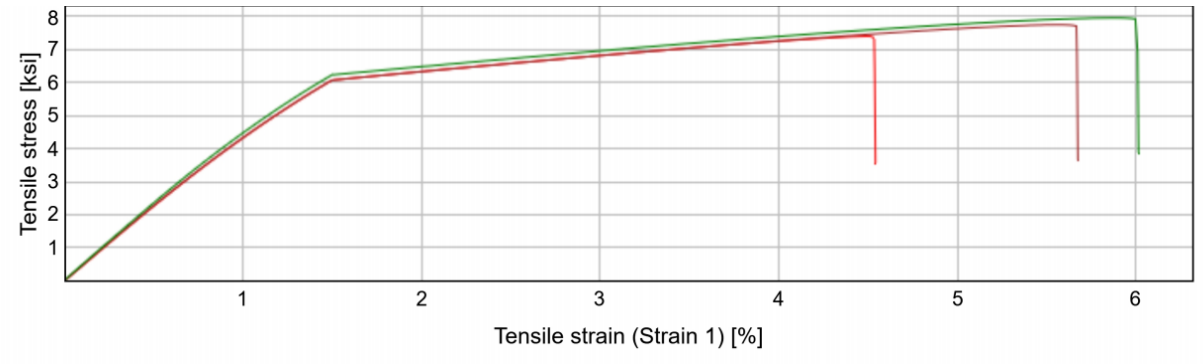

Figure 14: Test 2 Results [8].

In this third test, three distinct configurations were implemented. The initial configuration involved a blend of Gyroid and concentric patterns, with each layer consisting of 0.2 mm of concentric infill followed by 0.2 mm of Gyroid, repeating this sequence until the part reached a thickness of 3.4 mm. The second configuration combined concentric and cubic infill patterns, while the third configuration featured a mixture of honeycomb and concentric patterns. Each of the three setups began and ended with concentric infill, differing only in the intermediate layer patterns. Additionally, the spacing remained consistent across all configurations.

In the third test, the combination of honeycomb and concentric patterns displayed the highest tensile stress, reaching 6.366 ksi, with an ultimate tensile stress of 8.139 ksi. Conversely, the concentric and cubic infill combination demonstrated the lowest tensile stress in this test, registering at 5.923 ksi. This outcome likely resulted from the part's reduced resistance to stretching in the Y direction, attributed to the sharp corners formed by the cubic infill. As depicted in Figure 15 below, it is evident that the concentric infill combined with a honeycomb pattern yielded the highest tensile strength. Despite this, the other two designs still exhibited increased strength with an average of 6.009 ksi, surpassing that of concentric infill alone, which averaged 5.573 ksi. All three orientations fractured outside of the marked 1 in area and showed no measured elongation.

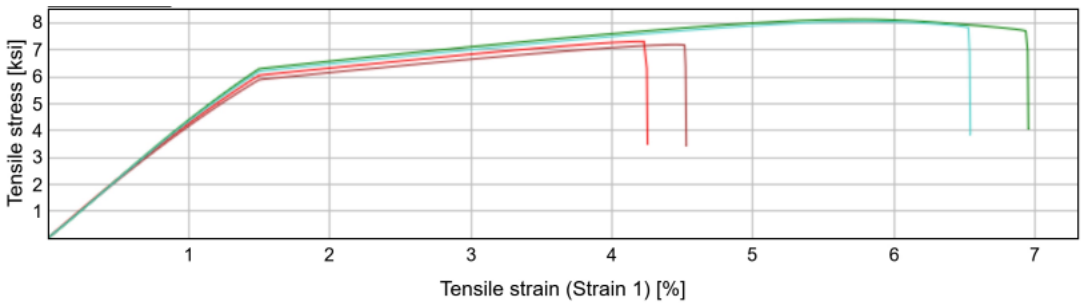

Figure 15: Test 3 Results [8].

The outcomes from the third experiment showcased the highest strength compared to previous iterations, closely resembling the configurations employed in test 3. However, notable distinctions include the use of concentric and rectilinear patterns instead of concentric and cubic. Furthermore, variations were introduced in other samples, such as increased infill in mid-layers; for example, the honeycomb/concentric variant featured thicker layers of honeycomb compared to its predecessor. This enhanced honeycomb/concentric design demonstrated a tensile stress of 6.526 ksi, slightly surpassing the 6.391 ksi exhibited by the concentric cubic counterpart. The consistent strength observed in these parts underscores the positive impact of refined infill patterns on overall structural integrity. Figure 16 pictured below illustrates the results of test 4, clearly demonstrated that the honeycomb/concentric design had the highest Tensile Stress.

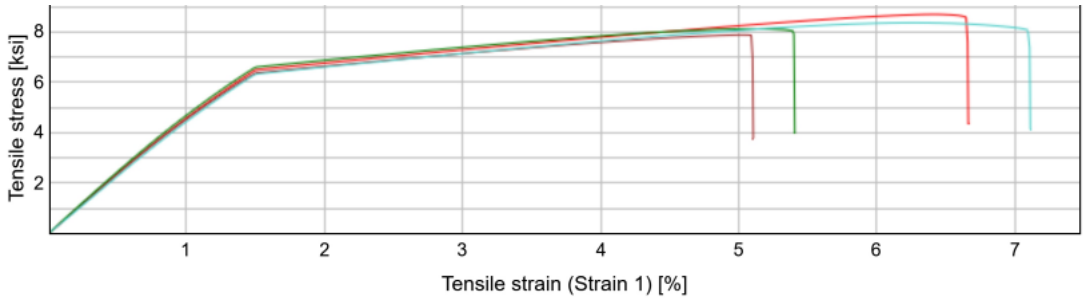

Figure 16: Lab 4 Results [8].

The conclusive tensile examination involved three novel configurations, each sharing similarities in the rectilinear infill pattern. However, the initial specimen featured a hybrid of concentric and rectilinear structures, the second one exclusively adopted a rectilinear pattern

with a modified fill angle ranging from 0^o to 45^o degrees on the outer layers and 90^o degrees on the inner layers. The ultimate sample combined concentric and rectilinear elements, with varying fill angles in both sections, mirroring the fill angle of the sample just mentioned.

During testing an issue with concentric infill was noticed. For the concentric infill pattern on the tensile sample, the Prusa slicer software automatically started each concentric line (seam) at the same point 6 cm away from the left side of the tensile sample. This meant that each layer was connected at this point. This point of connection of each infill line was the weakest point of each line as it was the place where the melted PLA was connected to an already cooling PLA line. The issue with this was that 6 cm into the sample was where stress was applied. This caused samples with mostly concentric infill to fracture 6 cm away from the edge. Because of this weakness, each of the samples exhibited minimal ductility and broke quicker than anticipated. Each sample was only as strong as the bonding between each infill line connection, which lead to lower strength values and no yielding, as the middle zone of each tensile sample, the 1-inch section in the middle used for extensometer measurement sustained minimal yielding before the connection point failed. After examining the Prusa software, there were no seam options to adjust the starting location of concentric samples, so to combat the problems with concentric, rectilinear infill was used instead to provide the high tensile strength of concentric infill without creating the connection point in the middle of the tensile sample.

The final test using the mixture of $0^o - 45^o$ angled rectilinear infill results revealed consistent values for tensile stress, ranging from 6.1 ksi to 6.32 ksi and ultimate stress ranging from 7.95 ksi to 7.99 ksi. The combination of 0 degree and 45-degree rectilinear infill displayed the highest Young's Modulus at 473.7 ksi, while the lowest modulus of 463.4 ksi was observed. All three samples exhibited remarkably similar characteristics, with an average change in length

of 0.014 inches. The final figure, depicted below as Figure 17, illustrates the resemblance among the various test specimens and highlights the superior strength of the 0/45-degree rectilinear pattern compared to the other infills tested.

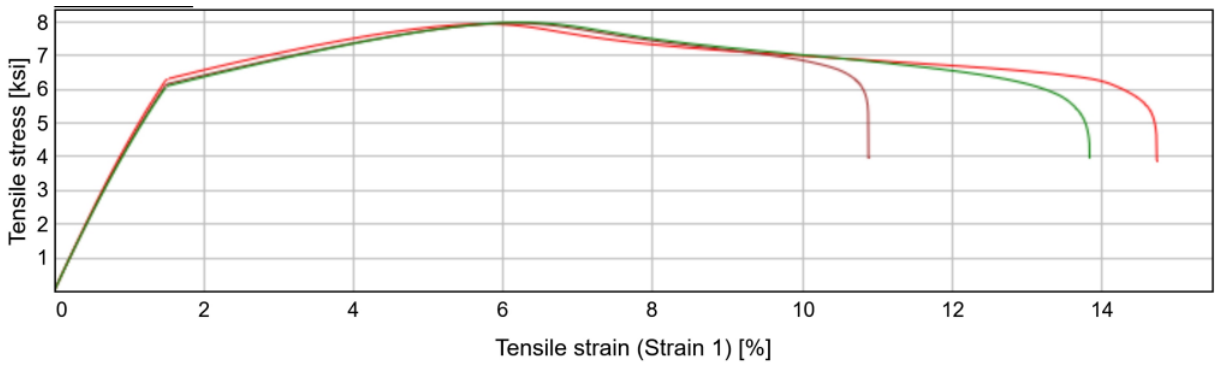

Figure 17: Final Test Results [6]

Final testing showed that the modified rectilinear infill pattern provided more strain compared to the modified concentric design without significantly compromising the strength. Shown in Figure 22, the modified 0 degree and 45-degree rectilinear infill produced a noticeable angle in the fracture compared to all the concentric infill designs, which produced brittle zero-degree breaks.

Conclusions

- Results for test 1 showed that for samples with concentric and grid infill patterns, there was a higher ultimate tensile stress for the concentric pattern, 6.788 ksi, compared to the grid pattern's average of 4.825 ksi.
- Results for test 2 showed that concentric infill patterns with added layers of angled rectilinear patterns at either the center of the sample or at the ends had an average tensile stress of 6.139 ksi for the three parts tested.
- Test 3 had 3 different samples configurations; a blend of gyroid and concentric patterns, combination of concentric and cubic infill patterns, and a mixture of honeycomb and concentric patterns. Gyroid and concentric patterns displayed a tensile stress of about 6 ksi. Concentric and cubic infill patterns displayed a tensile stress of 5.923 ksi. Honeycomb and concentric patterns displayed a tensile stress of 6.366 ksi.
- The design with honeycomb and concentric was enhanced in test 4 by thickening the layers, which resulted in a tensile stress of 6.526 ksi.
- The concentric infill pattern produced a defect 6 cm away from the left side of the print compromising the strength and ductility of the samples.
- Samples in the final test used rectilinear with 0- and 45-degree fill angles. Results for these samples showed that the ultimate stress ranged from 7.95 ksi to 7.99 ksi while the elongation was 0.014 inches on average.

References

[1] *What is tensile testing?*. TWI. (n.d.). https://www.twi-global.com/technical-knowledge/faqs/what-is-tensile-testing

[2] S. W., Hoag (n.d.). *Stress Strain Graph*. Research Gate. Retrieved September 18, 2022, from https://www.researchgate.net/figure/A-typical-stress-strain-curve-for-polymer-film-undergoing-tensile-strain-testing_fig6_236924185

[3] Prime. (2022, December 13). *PLA plastic: What is it and what is it used for?*. Prime Biopolymers. https://primebiopol.com/plastico-pla-que-es-y-para-que-se-utiliza/?lang=en

[4] O. S. Es-Said, R. M., J. Foyos, R. Noorani, M. Mendelson, & Pregger, B. A. (2000). Effect of Layer Orientation on Mechanical Properties of Rapid Prototyped Samples. *Materials and Manufacturing Processes*, *15*(1), 107–122. https://doi.org/10.1080/10426910008912976.

[5] Xometry, T. (2022, August 23). *Infill in 3D printing: Definition, Main Parts, and Different Types*. https://www.xometry.com/resources/3d-printing/what-is-infill-in-3d-printing/

[6] Moody, J., & Parenti, M. (2022, December 13). *Prusaslicer infill patterns: All you need to know*. All3DP. https://all3dp.com/2/prusaslicer-infill-patterns/

[7] Pranav. (2023, June 29). *What is the strongest infill pattern?*. Clever Creations. https://clevercreations.org/what-is-strongest-infill-pattern-cura-prusa/

[8] Minter, Tristan, Mechanical Engineering Department, Loyola Marymount University, Digital Images, 2023

[9] Es-Said, Lecture Notes, 2023

[10] Garcia, Antonio, Mechanical Engineering Department, Loyola Marymount University, Digital Images, 2023

Appendices

Appendix A

Photos of samples after undergoing tensile testing from all trials. All samples used PLA filament and were printed on a Prusa i3 MK3S printer and tested on an Instron 4505 UTS.1

Figure 18: Trial 1 Samples after Tensile Testing [8].

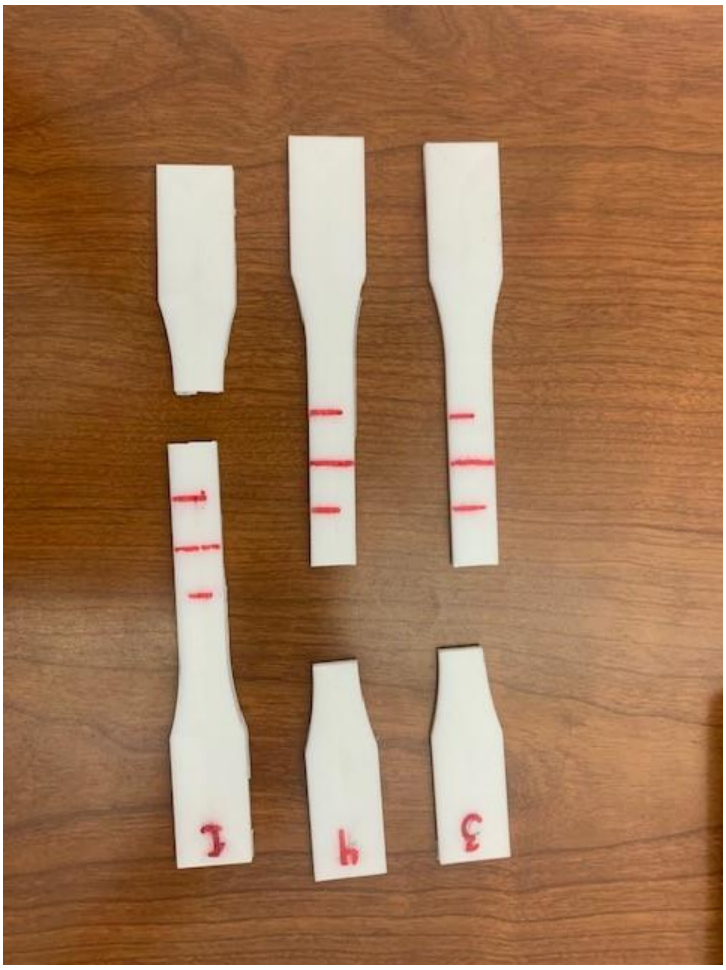

Figure 19: Trial 2 Samples after Tensile Testing [8].

Figure 20: Trial 3 Samples after Tensile Testing [8].

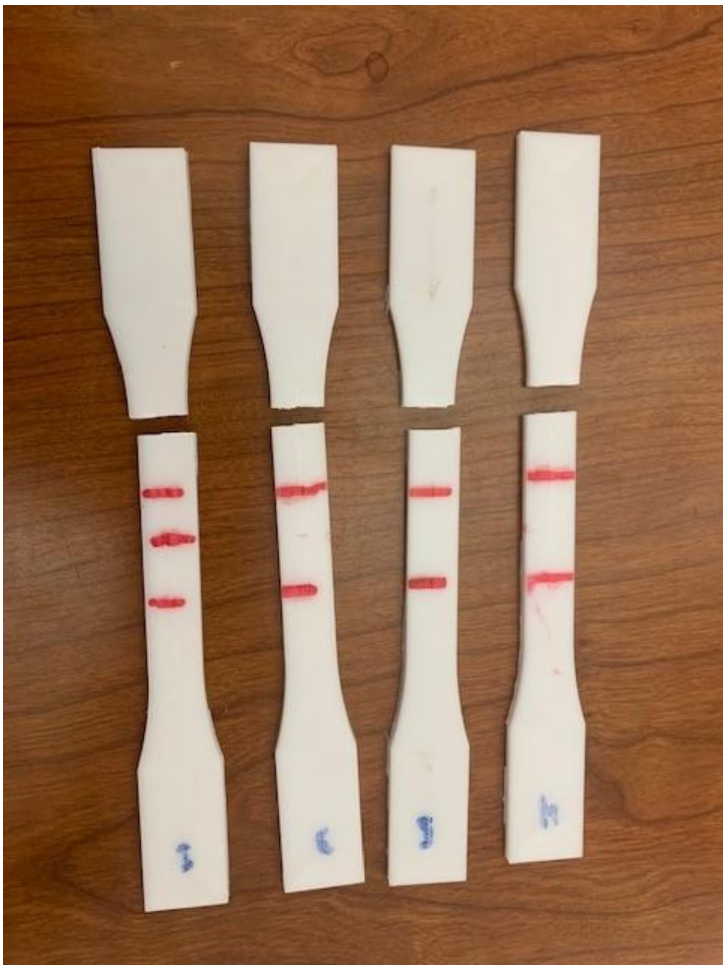

Figure 21: Trial 4 Samples after Tensile Testing [8].

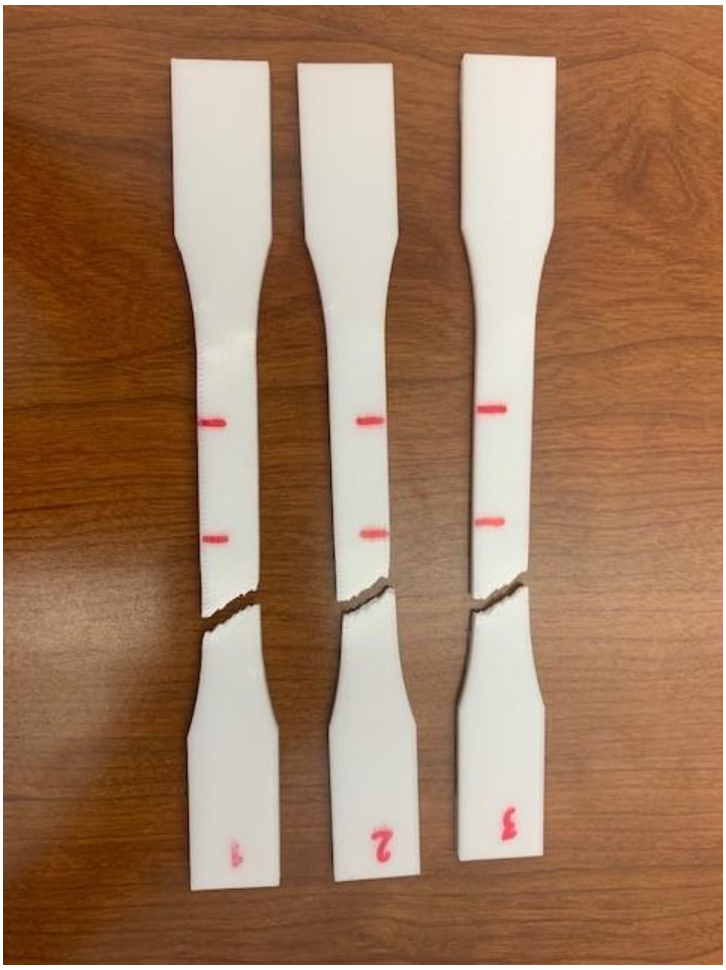

Figure 22: Trial 5 Samples after Tensile Testing [8].

Appendix B

Raw data taken from the Bluehill software of each sample's size and tested yield stress, ultimate stress, and Youngs Modulus. This data was recorded by following the experiment procedure found on page 8. The data found varies from each design as expected. Changes in infill pattern affected the overall mechanical properties of the tensile sample by either increasing the strength of the sample or increasing the ductility. For trials 1-4 no percent elongation was observed.

Specimen Label (Infill)	Tensile Stress at Yield (Offset 0.2%) [ksi]	Ultimate Tensile Stress [ksi]	Modulus (Automatic Young's) [ksi]	Width [in]	Thickness [in]
Tristan T1 (Grid)	5.480	6.617	464.008	0.508	0.131
Tristan T2 (Grid)	5.665	6.958	453.646	0.504	0.131
Tristan T3 (Grid/Concentric)	4.180	4.711	425.236	0.508	0.134
Tristan T4 (Grid/Concentric)	4.378	4.938	398.336	0.501	0.133

Table 1: Raw data from Trial 1 [10].

Specimen Label (Infill)	Tensile Stress at Yield (Offset 0.2%) [ksi]	Ultimate Tensile Stress [ksi]	Modulus (Automatic Young's) [ksi]	Width [in]	Thickness [in]
Tristan T5 (Modified Concentric at edges)	6.089	7.399	457.383	0.496	0.134
Tristan T6 (Modified Concentric at center)	6.089	7.748	458.566	0.496	0.134
Tristan T7 (Modified Concentric at center)	6.243	7.956	471.135	0.500	0.133

Table 2: Raw data from Trial 2 [10].

Specimen Label (Infill)	Tensile Stress at Yield (Offset 0.2%) [ksi]	Ultimate Tensile Stress [ksi]	Modulus (Automatic Young's) [ksi]	Width [in]	Thickness [in]
Tristan T8 (Concentric/Cubic Mix)	6.095	7.315	446.657	0.499	0.133
Tristan T9 (Concentric/Cubic Mix)	5.923	7.199	441.236	0.494	0.136
Tristan T10 (Concentric/Honeycomb Mix)	6.366	8.139	454.500	0.499	0.134
Tristan T11 (Concentric/ Honeycomb Mix)	6.266	8.064	447.359	0.500	0.134

Table 3: Raw data from Trial 3 [10].

Specimen Label (Infill)	Tensile Stress at Yield (Offset 0.2%) [ksi]	Ultimate Tensile Stress [ksi]	Modulus (Automatic Young's) [ksi]	Width [in]	Thickness [in]
Tristan 12 (2/3 Concentric and 1/3Rectilinear Mix)	6.526	8.702	482.965	0.499	0.132
Tristan 13 (Modified Concentric)	6.391	7.883	481.886	0.494	0.132
Tristan 14 (Modified Concentric)	6.624	8.124	496.695	0.494	0.130
Tristan 15 (Concentric/ Honeycomb Mix)	6.387	8.370	456.794	0.498	0.132

Table 4: Raw data from Trial 4 [10].

Specimen Label (Infill)	Tensile Stress at Yield (Offset 0.2%) [ksi]	Ultimate Tensile Stress [ksi]	Modulus (Automatic Young's) [ksi]	Width [in]	Thickness [in]
Tristan 16 (Modified Rectilinear)	6.319	7.946	473.698	0.504	0.133
Tristan 17 ((Modified Rectilinear)	6.169	7.971	465.457	0.506	0.132

Tristan 18 (Modified Rectilinear)	**6.105**	**7.989**	**463.397**	**0.500**	**0.132**

Table 5: Raw data from Trial 5 [10].

Appendix C

Appendix C shows all print setups. All prints were set up using Prusa Slicer and printed on a Prusa i3 MK3S printer, using a white PLA filament.

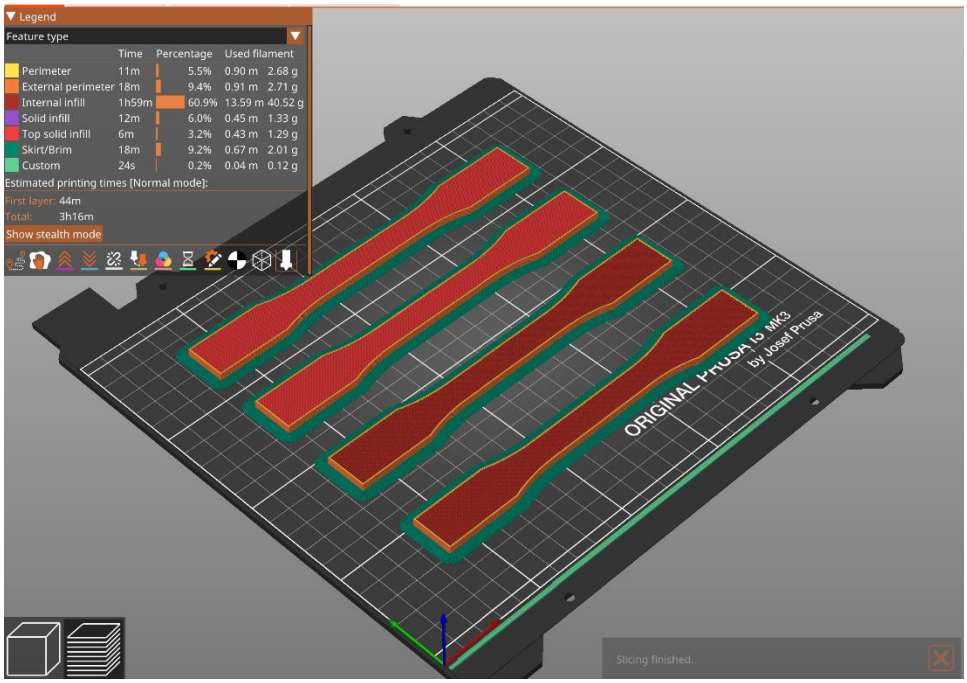

Figure 23: Trial 1 Board Setup [8].

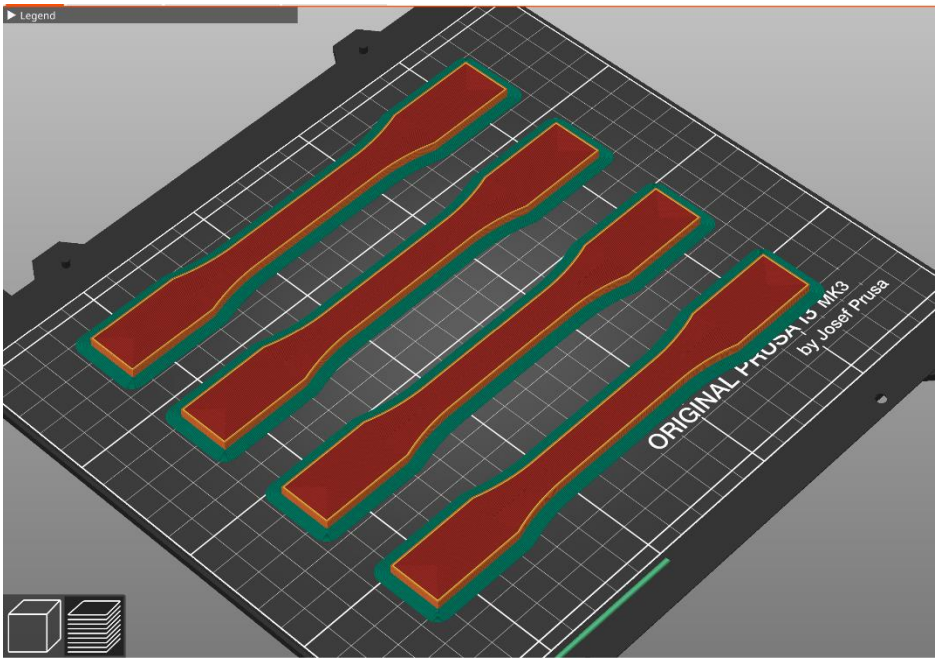

Figure 24: Trial 2 Board Setup [8].

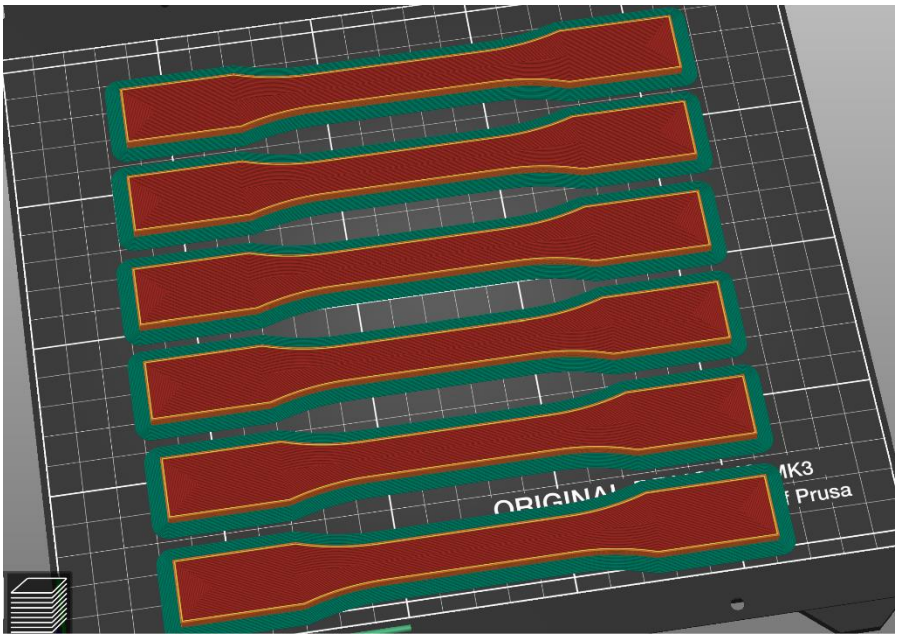

Figure 25: Trial 3 Board Setup [8].

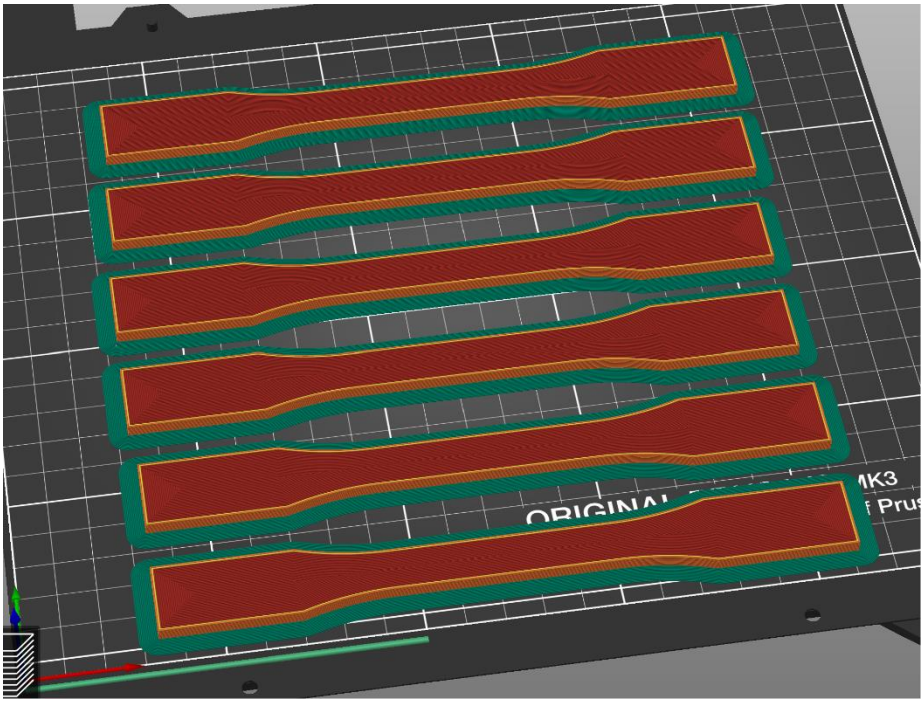

Figure 26: Trial 4 Board Setup [8].

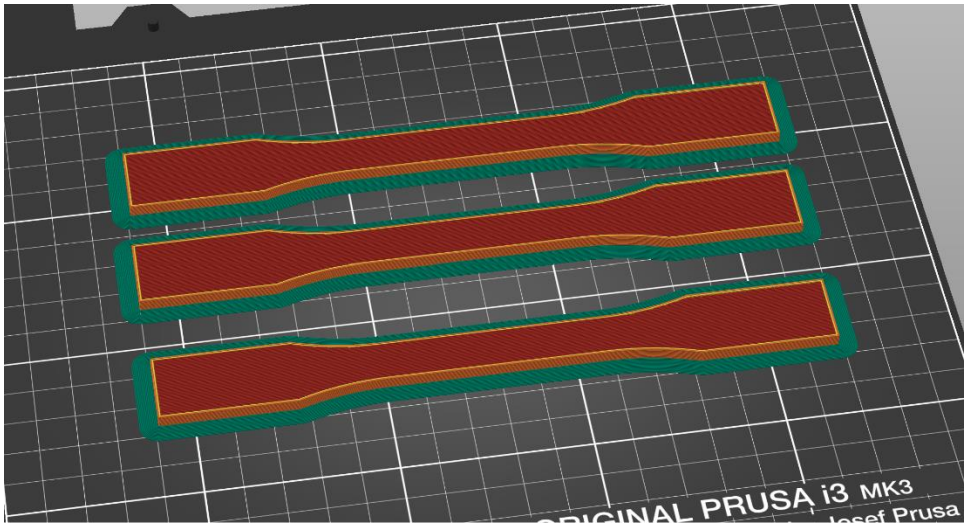

Figure 27: Trial 5 Board Setup [8].